*Proceedings World Geothermal Congress 2000*
*Kyushu - Tohoku, Japan, May 28 - June 10, 2000*

# SELF-POTENTIAL SURVEY IN THE MATALOKO GEOTHERMAL PROSPECT, FLORES, INDONESIA.

Kasumi Yasukawa[1] , Achmad Andan[2], Dendi S. Kusuma[2] and Toshihiro Uchida[1]

[1] Geological Survey of Japan, 1-1-3 Higashi, Tsukuba, Ibaraki 305-8567, Japan
[2] Volcanological Survey of Indonesia, Jl. Diponegoro No. 57 Bandung, Indonesia

**Key words:** self-potential, Mataloko, Indonesia, numerical modeling

**ABSTRACT**

A self-potential (SP) survey was carried out in the Mataloko geothermal prospect, Flores Island, Indonesia. The highest positive SP anomaly was observed at the main geothermal manifestation area. The extent of the positive SP anomaly zone corresponds with the hot-spring areas in a low-resistivity zone. In order to estimate the extent of the high-permeability zone around the hot-spring area, a two dimensional numerical modeling was done with a coupled fluid flow and SP simulator. Rough estimation of the permeability distribution was thus derived by matching the calculated and the observed SP profiles.

## 1. INTRODUCTION

SP surveys have been widely conducted in many geothermal fields assuming that the main cause of the anomaly is streaming potential. Most of these data have been interpreted qualitatively; a positive SP anomaly often indicates an upflow zone and the negative may indicate a downflow zone (Ishido, 1989). However the exact location of these flow zones do not necessarily correspond to the highest or lowest SP anomaly because of the subsurface inhomogeneity which even causes negative SP anomalies at upflow zones (Ross and Blackett, 1995, Sill, 1983, etc.). Some authors introduce quantitative SP analysis by representing the origins of the SP anomaly as sets of electrical current sources within a resistivity model (Corwin and Hoover, 1979, Fitterman, 1979, etc.). However such an approach doesn't describe the fluid flows that give rise to the current sources. Therefore an SP data analysis considering hydrological and electrical structures is essential for its detailed interpretation.

The first half of this paper explains the SP survey in the Mataloko geothermal area. The later part presents a two dimensional numerical model of fluid flow and its induced SP along a survey line to show the effectiveness of SP data analysis for geothermal reservoir exploration.

## 2. MATALOKO GEOTHERMAL PROSPECT

Mataloko geothermal area is located in the middle of Flores Island, Nusa Tenggara, Indonesia (Figure 1). Active volcanoes Inerie and Inerika are located in the south and the north of Mataloko, respectively. The basin between these volcanoes has an extent of 10 km in NNW-SSE direction. The older volcanoes occur at the edge of this basin while the younger ones are common in the inner part of the basin. This basin is considered to be a caldera.

Surface manifestations of geothermal steam and hot springs can be observed in the Mataloko area where the elevation is around 1000m. The main manifestation area is located in the valley along a stream named Wae Luja. Some alteration zones also exist around this river.

The Volcanological Survey of Indonesia (VSI) has conducted geological, geochemical and geophysical surveys in Flores island. New Energy and Industrial Technology Development Organization (NEDO) and Geological Survey of Japan (GSJ) have been engaged in a research project with VSI since 1997 and started surveying the Mataloko geothermal prospect in 1998.

## 3. SP SURVEY IN MATALOKO

An SP survey in Mataloko was conducted in July, 1998, around the stream of Wae Luja, across the alteration zones identified by geological surveys. The total number of the SP measurement points is 430 with a spacing of 100 m along survey lines. The covered area is about 5 km in the E-W and 6.5 km in the N-S directions.

Figure 2 shows the location of the SP survey points in Mataloko area. The electric potential at a survey point *P1* is assumed to be zero. Loop corrections were applied to measured SP data. Figures 3 and 4 show the resultant SP profiles along *P*- and *V*- survey lines, respectively. Dotted lines represent raw SP values and solid ones show the SP value after loop corrections. Figure 5 is a contour map of corrected SP in the Mataloko main area.

The highest SP anomaly in the Mataloko area is at *P36* in the main manifestation area along *P*- and *V*- lines. On *P*-line, which goes across Wae-Luja, a spike of SP anomaly was observed. This positive anomaly is limited only to the vicinity of the stream. On *V*-line which goes along the stream, a rather smooth slope was observed in the east (left side in Figure 4) but a steep drop occurs to the west of the highest anomaly. This suggests that surface manifestations may be present east of *P36* . This result is consistent with the fact that there are some hot springs in the east but none have been observed in the west.

A large negative anomaly, not corresponding to the topography, was observed around *Y8* east of the main manifestation area. An SP profile across this zone is numerically analyzed in the next section. Another negative anomaly around *S1* in the south corresponds with the location of a fault suggested from a gravity survey (Andan *et al.*, 1997). The other SP profiles are rather flat and the main causes of the anomalies are topographic effects or artificial noise around residential areas.

## 4. TWO DIMENSIONAL MODELING OF SUBSURFACE FLUID FLOW AND SURFACE SP

A two-dimensional SP model was completed along an E-W survey line (line-*C′* in Figure 5) with a coupled fluid flow and SP simulator *PTSP* (Yasukawa et al, 1993). Line-*C′* is located approximately 500m north of a resistivity survey line-*C* conducted by VSI (Andan et al, 1997) which crosses the main manifestation area. The solid line in Figure 6 shows the observed SP profile along line-*C′*. This SP profile is totally different from the pattern expected from its topography; the higher the elevation, the lower the SP. Therefore several effects of inhomogeneity of physical properties must be present.

In *PTSP*, temperature and pressure distributions in a system are calculated based on the energy and mass conservation equations for proper boundary conditions. The distribution of fluid velocity is thus obtained and the current source distribution caused by fluid flow is calculated for a given electro-kinetic cross-coupling conductivity as follows;

$$S = -\nabla L_V \cdot \boldsymbol{u} - L_V \nabla \cdot \boldsymbol{u} \qquad (1)$$

where $S$ , $L_V$ and $\boldsymbol{u}$ are electrical current per unit volume (Amp/m$^3$), velocity cross-coupling conductivity (Amp-sec/m$^3$) and velocity field (m/sec), respectively. The induced SP distribution is then calculated for a given resistivity structure. Therefore input data of permeability, resistivity and cross-coupling conductivity distribution, in addition to boundary conditions are required for the calculation by *PTSP*. For more details, see Yasukawa *et al.* (1993).

Note that the temperature dependence of cross-coupling conductivity is automatically calculated in *PTSP*. According to Sill (1983), the variation of $L_V$ with temperature $T$ below 300 $^o$C is approximately described by;

$$L_V(T) = L_{V0}(1 + C\Delta T), \quad \Delta T = T - T_0 \qquad (2)$$

where $C$ is a constant and subscript 0 indicates the reference temperature $T_0$ . This equation is introduced in *PTSP* with the constant $C = 0.01$ ($^o$C$^{-1}$), which is consistent with the experimental results of Ishido and Mizutani (1981), as well as those of Morrison *et al.* (1978).

Figure 7 shows the resistivity and permeability grids of the numerical model. The resistivity grid is based on the result of resistivity surveys conducted by VSI (Andan et al., 1997). A low resistivity layer (5 ohm-m) reaches to a shallower depth at the vicinity of Wae-Luja. Since a negative SP anomaly on a topographic slope can not result from a resistivity structure alone (Yasukawa and Mogi, 1998), a permeability model was also introduced. At first a permeability model with the same geometry as the resistivity was applied; for the lower resistivity layer a higher/lower permeability was given. However, no high SP anomaly was calculated for this layered permeability model. Therefore a vertical contact model was considered; a higher permeability column was assumed near the negative anomaly zone. A lower permeability column was also tested, but the negative anomaly in Figure 6 can be reconstructed only by a higher permeability model. The width and the contrast of the high permeability zone was adjusted until the resulting SP profile showed a good match with the observations.

For the fluid flow calculation, the following boundary conditions were assumed; a constant pressure and temperature surface (1 atm, 20 $^o$C), impermeable side boundaries and a constant temperature bottom (70 $^o$C) which gives a normal geostatic temperature gradient. $L_{V0}$ is assumed to change with permeability because its variation is mainly caused by the chemical components which change is considered to be small in a single reservoir.

Figure 6 shows the comparison of the observed and calculated SP. A quite good match was obtained for this grid size (100x100 m$^2$). High frequency anomalies in the observed SP are probably caused by the shallower features.

The location of the high permeability zone is consistent with the fact that no hot springs occur west of *P1* while some hot springs are present east of *P1*. However, since the fluid in this zone flows downward according to the fluid flow simulation, the surface manifestations are considered to be quite local phenomena and the most part of the high permeability zone is a downflow zone. A big negative SP anomaly along line-*C′* is thus caused by the downflow.

## 5. DISCUSSIONS

The uniqueness of the resistivity and permeability models shown in this study has not been established. The sensitivity of the vertical extent of the high permeability zone will be investigated in the next stage. However, SP numerical modeling suggests the existence of a high permeability zone and its surface extent. A combination of resistivity and SP surveys is used for investigation of the permeability structure.

This SP modeling was performed assuming the SP anomaly is caused only by topography, resistivity and permeability structures; no hot fluid source was assumed because there is no clear surface manifestation along line-*C′*. For more sophisticated modeling, a survey line across the main manifestation should be selected for the modeling so that the hot fluid flow from a depth can be considered. The effect of three dimensional structure will also be investigated.

## 6. CONCLUSIONS

An SP survey has been conducted in the Mataloko geothermal area. The highest positive anomaly was observed in the main geothermal manifestation area along the stream Wae-Luja which flows eastward. SP values drastically drop toward the north, south and west while they gradually decrease toward the east. Its location is consistent with the fact that some hot springs occur only in the east of the main manifestation area. A local negative SP anomaly found in the southern area corresponds to a fault zone suggested from gravity data.

A two-dimensional hydrological and electrical structure model was numerically constructed for an east-west cross-section. The permeability structure of this model was determined by a trial-and-error method to obtain a good match with the observed data while the resistivity structure used is determined from the resistivity survey. The resultant permeability model suggests the existence of high permeability zone around the main manifestation area.

## ACKNOWLEDGMENTS

Note that this study is a part of the Japan-Indonesia cooperative research project "the exploration of small-scale geothermal resources in the eastern part of Indonesia" conducted by Geological Survey of Japan, New Energy and Industrial Technology Development Organization and Volcanological Survey of Indonesia.

## REFERENCES

Andan, A., Suhanto E., Sukirman, A., Ashari and Usmawardi (1997). *Report on integrated geophysical investigation of Mataloko geothermal area, Ngada 2nd regency, Nusa Tenggara, Timur province.* VSI Report, 46pp.

Corwin, R. F. and Hoover, D. B. (1979). The self-potential method in geothermal exploration. *Geophysics*, Vol. 44 (2), pp. 226-245.

Fitterman, D. V. (1979). Calculations of self-potential anomalies near vertical contacts, *Geophysics*, 44 (2), pp. 195-205.

Ishido, T. (1989). Self-potential generation by subsurface water flow through electrokinetic coupling, Lecture notes in earth sciences, 27, *Detection of subsurface phenomena*, Springer-Verlag, Berlin.

Ishido, T. and Mizutani, H. (1981). Experimental and theoretical basis of electrokinetic phenomena in rock-water systems and its application to geophysics, *J. Geophys. Res.*, Vol. 86, pp. 1763-1775.

Morrison, F., Corwin, R. F., De Moully, G. and Durand, D. (1978). *Interpretation of self-potential data from geothermal areas*, Semi-annual technical report, Contract #14-08-0001-16546, Sponsored by U.S.G.S.

Ross, H. P., Blackett, R. E., and Witcher, J. C. (1995). The Self-Potential method: Cost-effective exploration for moderate-temperature geothermal resources, *Proceedings, World Geothermal Congress, Florence, Italy*, Vol. 1, pp. 645-648.

Sill, W. R. (1983). Self-Potential modeling from primary flows, *Geophysics*, Vol. 48 (1), pp. 76-86.

Yasukawa, K., Bodvarsson, G.S., Wilt, M. (1993). A coupled self-potential and mass-heat flow code for geothermal applications, *GRC Transactions*, Vol. 17, 203-207.

Yasukawa, K. and Mogi, T. (1998) Topographic effects on SP anomaly caused by subsurface fluid flow—numerical approach—. *BUTSURI-TANSA*, 51 (1), pp. 17-26 (in Japanese).

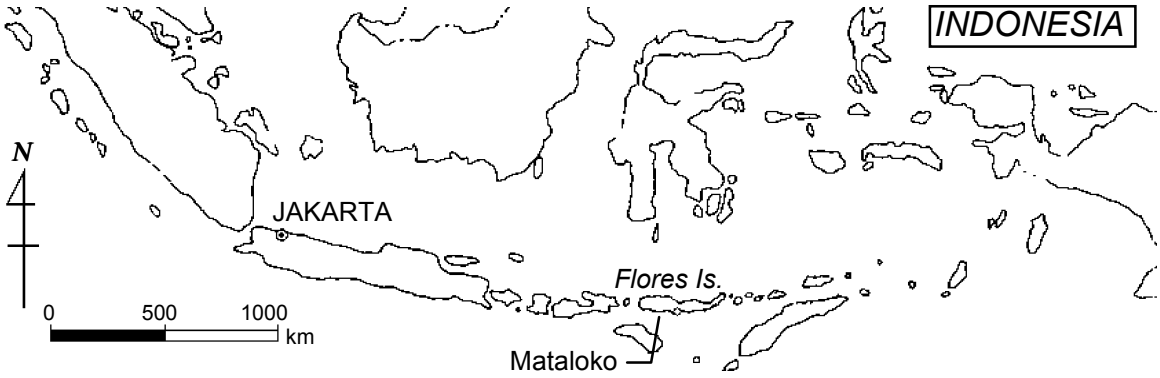


Figure 1. Location of the Mataloko geothermal area.

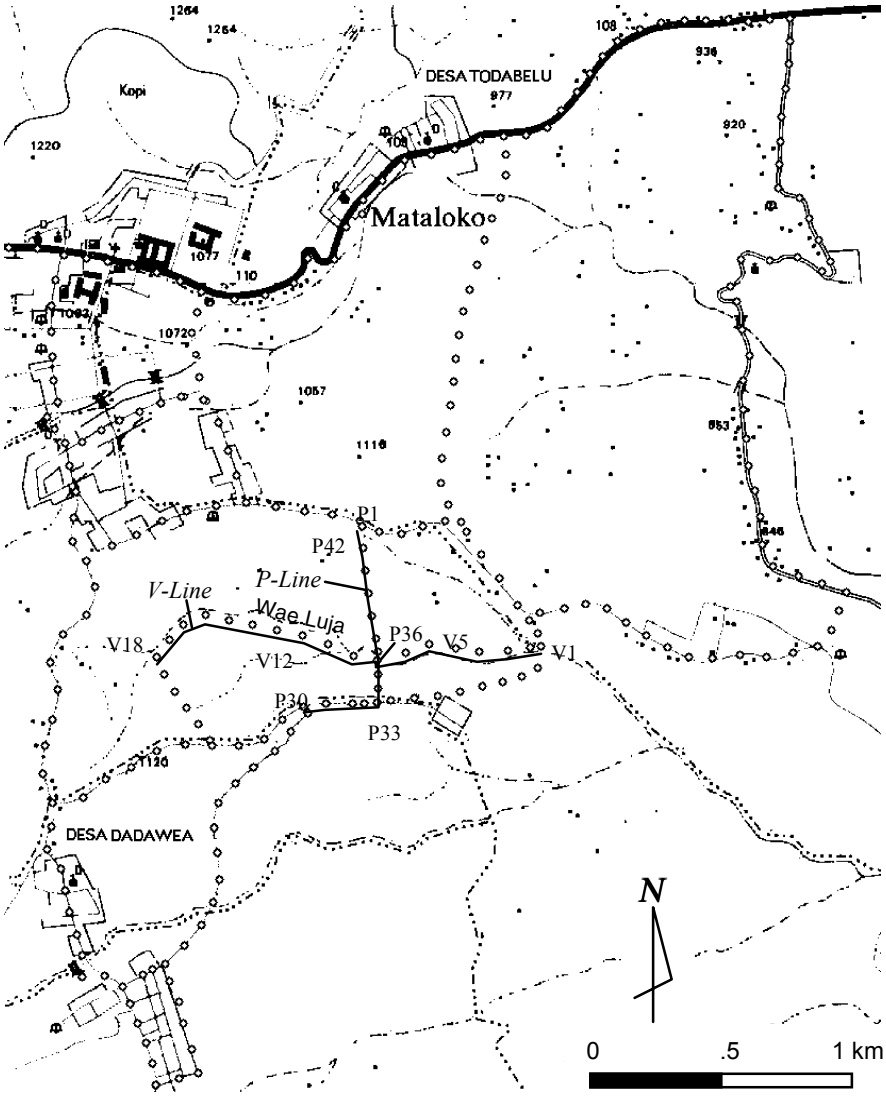


Figure 2. SP survey points (o) in the Mataloko area in 1998.

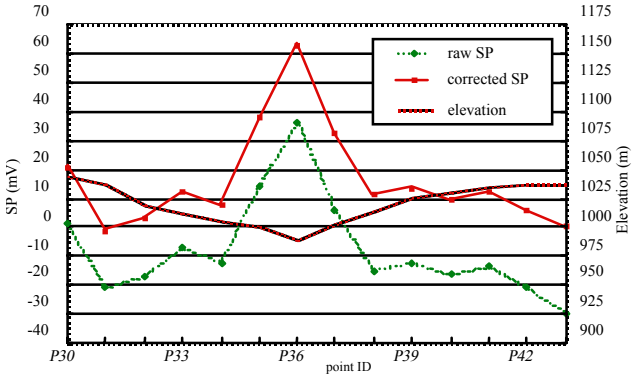


Figure 3. Observed SP and elevation profiles; *P*-line.

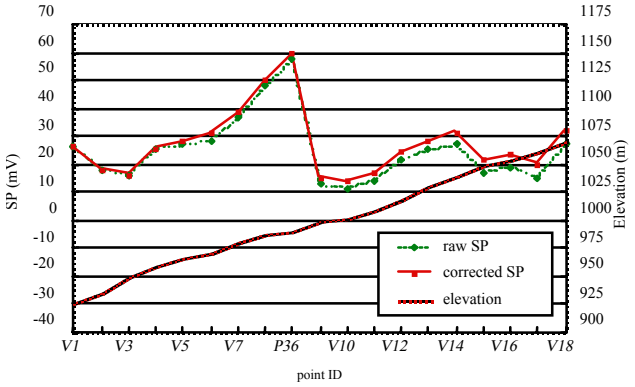


Figure 4. Observed SP and elevation profiles; *V*-line.

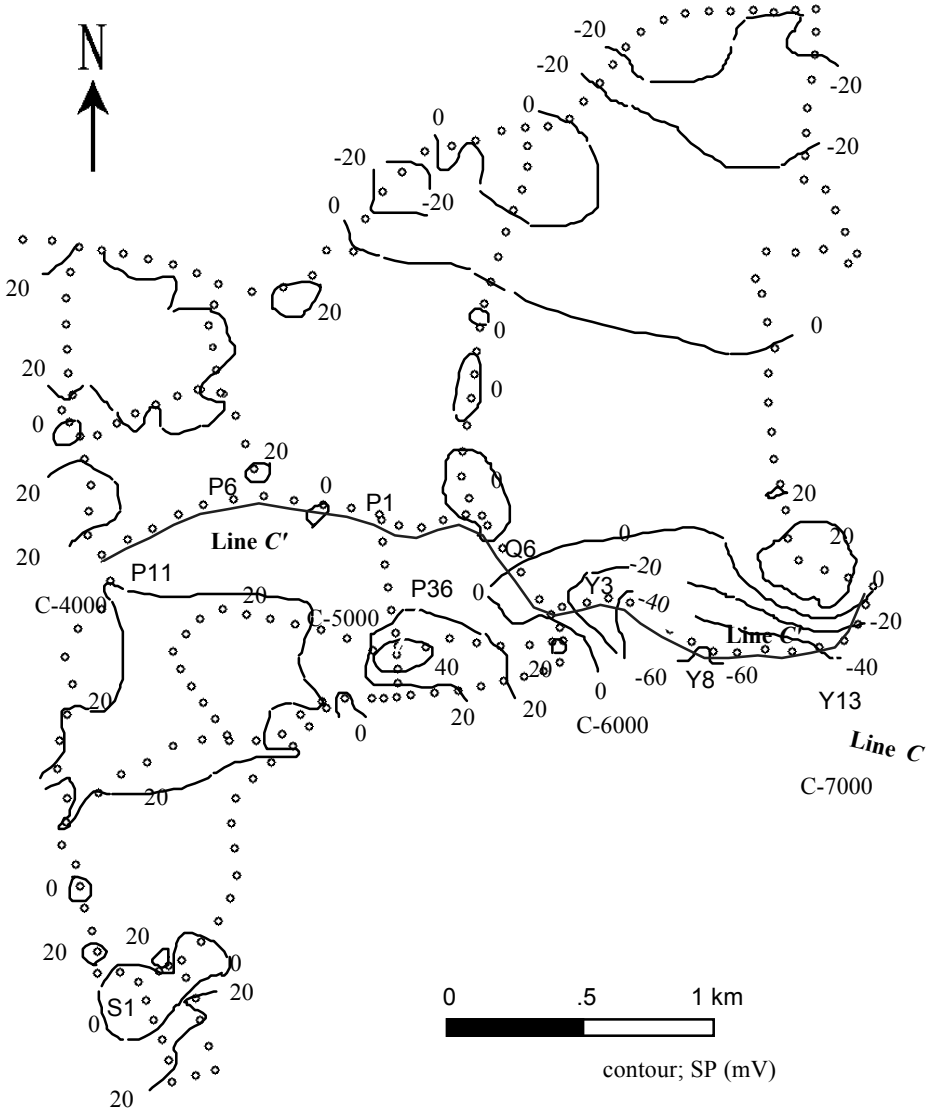


Figure 5. SP distribution in the Mataloko area.

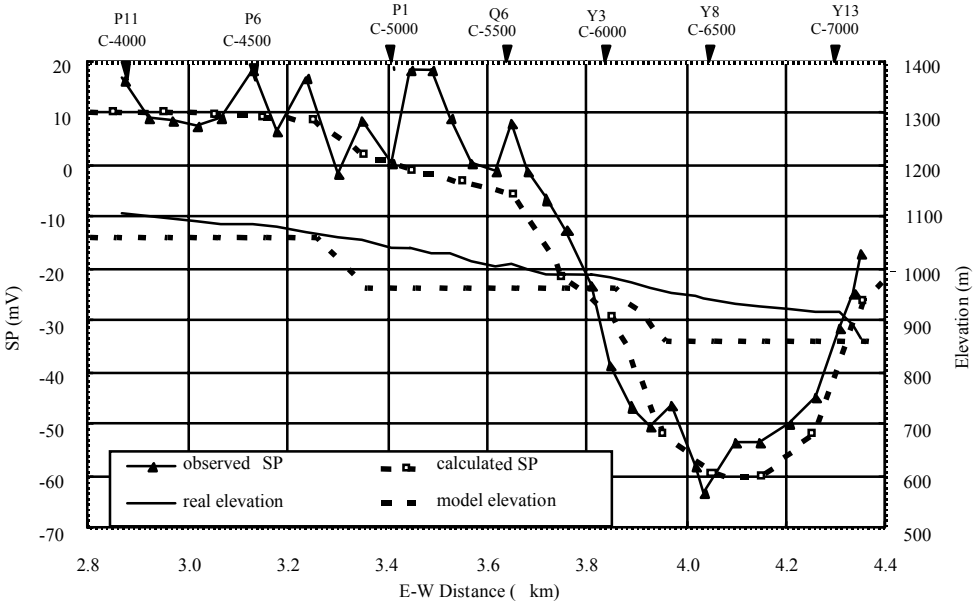


Figure 6. Comparison of observed and calculated SP profiles along line-*C′*.

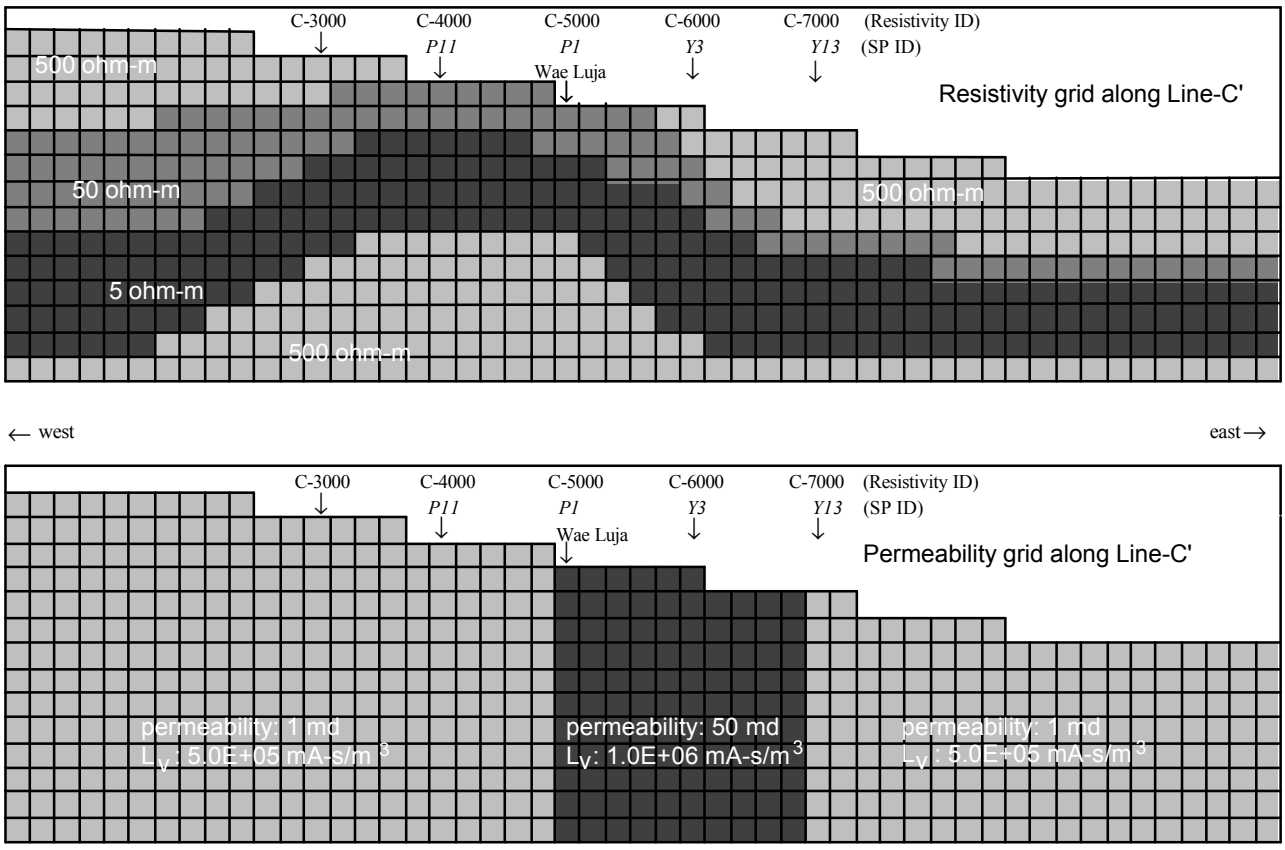


Figure 7. Physical property grids of the model.